Supporting Information for:

Attapulgite–Polysulfide Composite for Highly Selective, Scalable Recovery of Precious Metals from Gold Ore Residues and Wastewater

Shu-Juan Wang, [a] Yong-Jun Ma, [a] Xiao-Jun Liu, [a] Xi-Cun Wang, [a] Xiao-Feng Wu,[*b] and Zheng-Jun Quan,[*a]

[a] College of Chemistry and Chemical Engineering, Northwest Normal University, Lanzhou 730070, Gansu, China. E-mail: quanzhengjun@hotmail.com

[b] Department of Chemistry, University of Liverpool, Liverpool, UK L69 7ZD. E-mail: xfwu@liverpool.ac.uk

Table of Content

1. Experimental Section

1.1 Synthesis of Poly(S-AM)

S_8 (500 mg, 1.95 mmol) and $Zn(DTC)_2$ (10 mg, 0.03 mmol) were placed into a 25 mL reaction tube equipped with a magnetic stir bar. The tube was connected to an exhaust gas treatment device and heated in a constant-temperature timing magnetic stirrer at 135°C. After S_8 was completely melted, AM (500 mg, 7.03 mmol) was added in batches. The stirring speed was set to 800 rpm. After reacting for 24 hours, the product in the reaction tube solidified completely. The heating was stopped, and the mixture was allowed to cool naturally to room temperature. The product was scraped out using a spatula, washed with ethanol, and then dried in a vacuum oven at 60°C for 8 hours to obtain a dark brown solid, Poly(S-AM). The resulting copolymer was thoroughly ground in an agate mortar. Subsequently, a series of copolymers Poly(S_x-AM_γ) with different ratios were prepared by varying the feed ratios, where x represents the mass fraction of S_8 and y represents the mass fraction of AM.

Gel Permeation Chromatography (GPC) Characterization： We thank the reviewer for raising this important point. The polymer we prepared showed poor solubility in other common solvents, thus gel permeation chromatography (GPC) in DMF was used to determine the number-average molecular weight (M_n) and weight-average molecular weight (Mw). However, these data require careful interpretation. As reported by Hasell and co-workers (Chem. Mater. 2022, 34, 1167−1178), polar amide solvents such as DMF, DMAc, and NMP can facilitate homolytic cleavage of polysulfide linkages (S-S bonds with a sulfur rank of three or higher), leading to partial degradation of sulfur-rich polymers during dissolution. This effect was confirmed by model compound studies, which demonstrated that trisulfides undergo rapid metathesis in DMF at room temperature, whereas disulfides remain stable under the same conditions.Consistent with this report, we attribute the three distinct molecular weight distributions observed in our GPC analysis to the in situ degradation of the polymer in DMF:

Highest molecular weight fraction (Peak 1): likely corresponds to residual segments that retained higher-rank polysulfide bonds or remained partially intact;

Intermediate molecular weight fraction(Peak 2): represents degradation products arising from partial chain scission;

Lowest molecular weight fraction(Peak 3): corresponds to smaller polymer species generated by extensive chain cleavage.

mer (Table S1).

Roman Characterization: The product was further analyzed by Raman spectroscopy (Figure S2). A distinct S–S stretching vibration peak was observed at approximately 455–495 cm^{-1}, confirming the formation of S–S bonds in the polymer. No significant C=C absorption peak was detected in the range of 1592–1614 cm^{-1}, indicating that the unsaturated double bonds of the olefin reacted with sulfur, leading to the disappearance of the double bonds. These results provide additional evidence for the successful synthesis of the Poly(S-AM) polymer.

^{1}H NMR Characterization: Poly(S-AM) was characterized by proton nuclear magnetic resonance (^{1}H NMR , Figure S3). The results showed that the olefinic proton signals of the acrylamide monomer at 5.6-6.3 ppm completely disappeared after polymerization, while new S-CH characteristic peaks appeared at 2.5-3.2 ppm. The amide proton peaks at 6.8-7.2 ppm remained after polymerization, indicating that the amide group did not participate in the reaction. Combined with the appearance of S-CH characteristic peaks and the formation of S-S bonds confirmed by Raman spectroscopy, it can be determined that acrylamide copolymerized with sulfur via its double bond rather than undergoing homopolymerization.

1.2 Acidification of Attapulgite (ATP)

ATP (10 g) was placed into a round-bottom flask. Then, 100 mL of 60% sulfuric acid was added. The reaction was carried out at 80°C with a stirring speed of 600 rpm for 2.5 hours. After the reaction was complete, the mixture was allowed to cool naturally to room temperature. The solid product was filtered, and the filter cake was washed with deionized water until the pH of the filtrate reached approximately 7. The solid was then dried in an oven at 100°C overnight to obtain the acidified and purified HATP.

2. Materials Characterization Methods

2.1 Structural Characterization

Fourier Transform Infrared Spectroscopy (FTIR): FTIR spectra were recorded on a Digilab FTS-3000 spectrometer (USA) in the spectral range of 400-4000 cm^{-1} to characterize the chemical functional groups.

X-ray Photoelectron Spectroscopy (XPS): XPS analysis was performed on a Thermo ESALAB 250XI spectrometer (USA) to determine the elemental composition, chemical states, and atomic concentrations on the surface of the polymers.

Powder X-ray Diffraction (PXRD): PXRD patterns of S_8, the polymers, and the composites were characterized on a Rigaku D/Max-2200PC diffractometer (Japan) using Cu Kα radiation (λ = 1.5418 Å) operated at 40 kV and 100 mA, with a scanning range of 5° to 80° (2θ).

Differential Scanning Calorimetry (DSC): DSC analysis was conducted on a TA Q2000 (USA) or a Discovery DSC25 instrument (TA Instruments) under a nitrogen atmosphere. The temperature program involved heating and cooling cycles from -50 to +150 °C at a constant rate of 10 °C min^{-1}.

Thermogravimetric Analysis (TGA): TGA was performed using a Mettler Toledo TGA/DSC1 analyzer (Switzerland) under a flowing nitrogen atmosphere. The samples were heated from 25 to 800 °C at a heating rate of 10 °C min^{-1}.

Scanning Electron Microscopy (SEM): The surface morphology of the polymers was observed using a ZEISS Sigma 300 field-emission scanning electron microscope.

Surface Area and Porosity Analysis (BET): The specific surface area and pore characteristics of the copolymers were determined using nitrogen adsorption-desorption isotherms at 77 K, asured with a Quantachrome EVO analyzer (USA). The Brunauer-Emmett-Teller (BET)

method was applied to calculate the specific surface area method was applied to calculate the specific surface area

Proton nuclear magnetic resonance (^{1}H NMR): The elemental composition and chemical shifts of the polymer were determined by nuclear magnetic resonance (NMR) spectroscopy using a Varian Mercury Plus 400 MHz spectrometer with DMSO-d_6 as the solvent.

Inductively Coupled Plasma Optical Emission Spectrometry (ICP-OES): The concentrations of metal ions in solutions before and after adsorption were measured and compared using an Agilent 5110 ICP-OES instrument (USA).

Sample	Mn (g mol^{-1})	Mw (g mol^{-1})	PD	Area (%)
Peak 1	71684	117485	1.64	6.0
Peak 2	1636	1957	1.20	29.3
Peak 3	463	492	1.06	`64.7

Table S1. GPC results of Poly(S-AM)

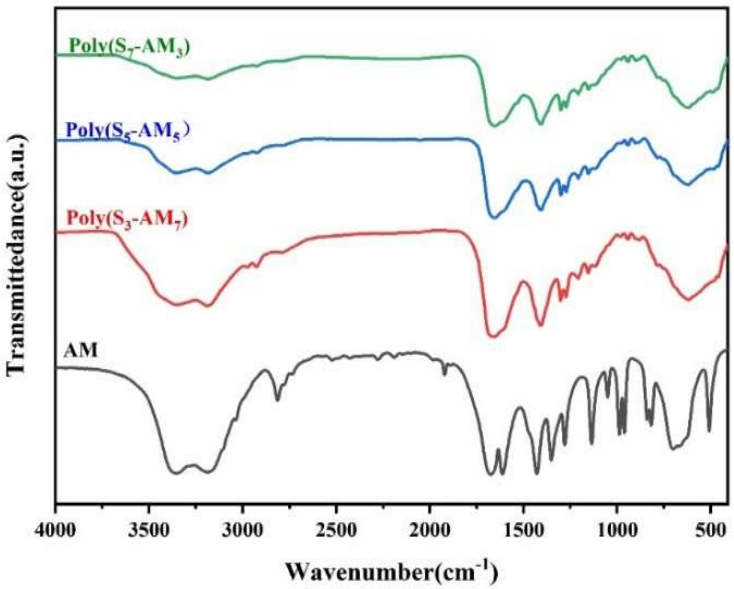

Figure S1 FT-IR spectra of P(S_x-AM_y) with different ratios

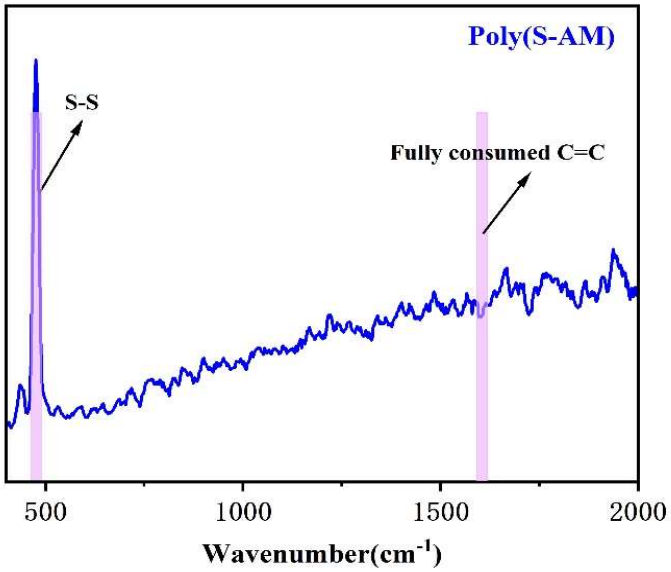

Figure S2 Raman Spectrum of Poly(S-AM)

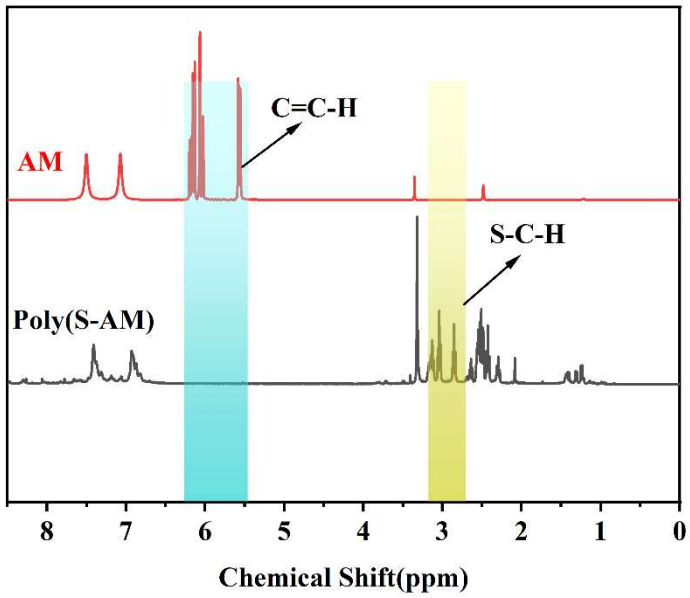

Figure S3 ^{1}H NMR spectra of AM and Poly(S-AM) in DMSO-d_6.

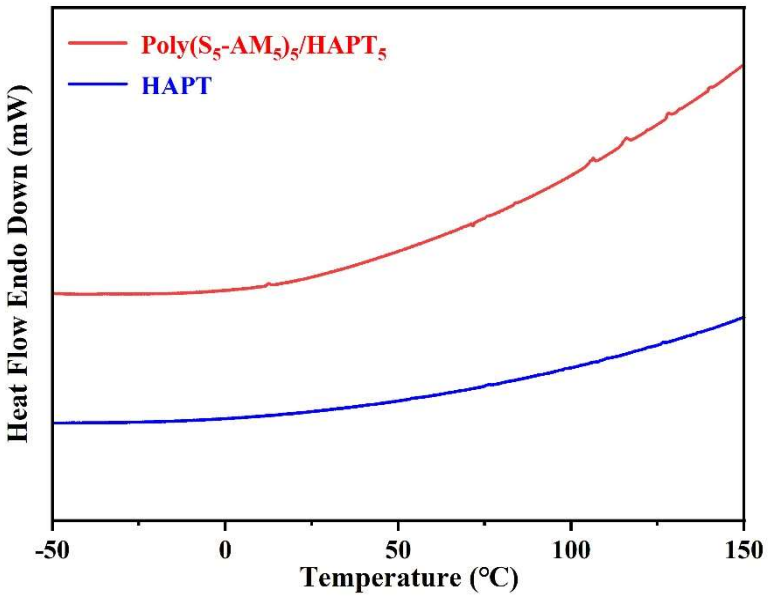

Figure S4 DSC thermograms of HAPT and Poly(S_5-AM_5)$_5$/$HAPT_5$.

2.2 Adsorption Performance Tests

2.2.1 Standard Calibration Curve for Au(III) Solution

A stock solution of Au(III) with a concentration of 1000 mg L^{-1} was diluted to prepare a series of standard solutions at different concentrations (e.g., 0 mg L^{-1}, 0.5 mg L^{-1}, 1 mg L^{-1}, 2 mg L^{-1}, 5 mg L^{-1}, 10 mg L^{-1}). The Au(III) concentration of each standard solution was measured using ICP-OES. A standard calibration curve was then established by plotting the measured intensity (or emission signal) against the known concentration, as shown in Figure S5.

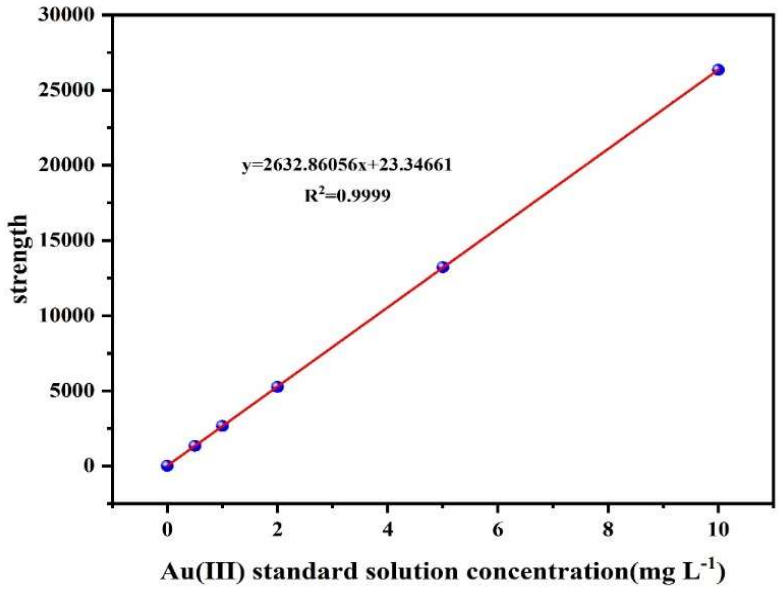

Figure S5 Standard calibration curve for Au(III) determination.

2.2.2 Effects of S_8 Content, Poly(S_5-AM_5) Content, and Initial Solution pH on Au(III) Adsorption Performance

(1) Effect of S_8 Content

To evaluate the effect of S_8 content, 2.5 mg of the prepared adsorbent material was added into 5 mL of Au(III) solution with an initial concentration of 600 mg L^{-1}. The mixture was then stirred for 12 hours at room temperature.

(2) Effect of Poly(S_5-AM_5) Content

To investigate the effect of Poly(S_5-AM_5) content, 2.5 mg of the prepared adsorbent material was added into 5 mL of Au(III) solution with an initial concentration of 500 mg L^{-1}. The mixture was stirred for 12 hours at room temperature.

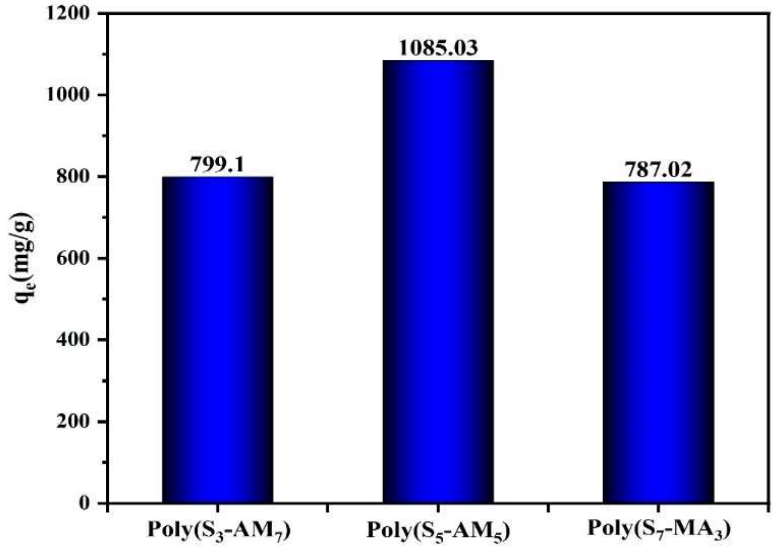

Figure S6 Adsorption performance of Poly(S-AM) with different ratios for Au(III).

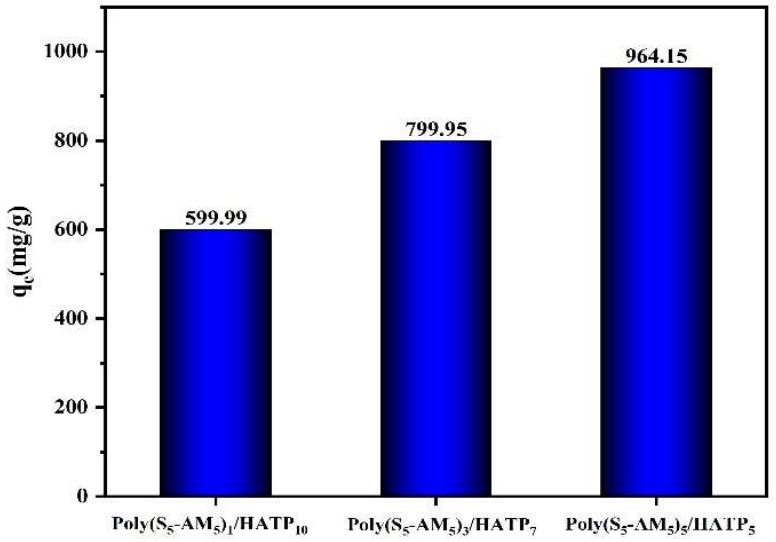

Figure S7 Adsorption performance of Poly(S_5-AM_5)$_x$/$HATP_y$ with different ratios for Au(III).

(3) **Effect of Initial Solution pH**

To assess the influence of initial solution pH on adsorption performance, 2.5 mg of the prepared adsorbent material was added into 5 mL of Au(III) solution with an initial concentration of 300 mg L^{-1}. The mixture was stirred for 12 hours at room temperature.

2.2.3 Adsorption Isotherm Experiments

To further investigate the adsorption mechanism, isothermal adsorption experiments were conducted. At room temperature, 2.5 mg of Poly(S_5-AM_5)$_5$/$HATP_5$ was added to 5 mL of Au(III) solutions with varying initial concentrations (60, 100, 200, 300, 400, 500, and 600 mg/L). The pH of each solution was adjusted to 1.0. The mixtures were stirred for 12 hours using magnetic stir bars. The effect of initial concentration on adsorption capacity is shown in Figure 3(a).

2.2.4 Adsorption Kinetics

Adsorption kinetic experiments were performed at room temperature. 2.5 mg of Poly(S_5-AM_5)$_5$/$HATP_5$ was added to 5 mL of a 500 mg L^{-1} Au(III) solution, and the pH was adjusted to 1.0. The mixture was stirred with a magnetic stir bar for predetermined time intervals (30, 60, 120, 240, 360, 480, 600, and 720 minutes). The results of the adsorption kinetic tests are presented in Figure 3(d).

2.2.5 Reusability Study

In practical applications, the reusability of an adsorbent is a crucial performance indicator. The regeneration process involves cycles of metal ion adsorption and desorption. For the adsorption step, the adsorbent was mixed with the metal ion solution in water and stirred at room temperature for 8 hours. The mixture was then centrifuged, the supernatant was removed, and the solid adsorbent (loaded with metal ions) was collected.

For desorption, the used adsorbent was treated with an eluent solution (8% hydrochloric acid and 10% thiourea), ultrasonicated for 30 minutes to promote desorption, and then centrifuged to collect the regenerated adsorbent. This recovered adsorbent was subsequently reused in the next adsorption cycle. This adsorption-desorption cycle was repeated seven times to evaluate the reusability performance.

A 0.20 g sample of gold mine tailings was weighed, moistened with a small amount of water, and then treated with 9 mL of aqua regia and 1 mL of hydrofluoric acid. The digestion vessel was tightly sealed and placed into the digester. Pre-digestion was performed at 120°C for 30 minutes, followed by microwave digestion according to the following program: 130°C with a

ramp time of 5 minutes and a hold time of 3 minutes; 150°C with a ramp time of 3 minutes and a hold time of 10 minutes; 180°C with a ramp time of 3 minutes and a hold time of 30 minutes. After cooling to 60°C, the digestate was diluted to 25 mL with deionized water, and the initial concentrations of metal ions were determined as shown in Table S4.

Table S2. Parameters of isotherm models for the adsorption of Au(III) onto Poly(S_5-AM_5)$_5$/$HATP_5$.

Langmuir			Freundlich		
q_m(mg/g)	K_L(L mg^{-1})	R^2	n	K_f(L mg^{-1})	R^2
961.54	17.02128	0.99999	6.59674	572.38395	0.48684

Table S3. Kinetic parameters for the adsorption of Au(III) onto Poly(S_5-AM_5)$_5$/$HATP_5$.

Pseudo-first-order-model			Pseudo-second-order-model		
qe(mg/g)	K1(g mg^{-1} min^{-1})	R^2	qe(mg/g)	K_2(g mg^{-1} min^{-1})	R^2
763.89	0.01241	0.95575	1004.69	0.00004	0.99959

Table S4. Initial concentrations of various metal ions in the gold ore residue leaching solution.

Sample mass m_0(g)	Fixed volumeV_0 (mL)	Elements tested	Concentration of elements in the test solution C_0(ug/L)	Dilution factor f	Element concentration in the original digestion solution C_1(ug/L)	Element content of the sample C_X(ug/ kg)
0.2016	25	Au	5.496	1	5.496	681.486
0.2016	25	Au	5.601	1	5.601	694.531
0.2016	25	Au	5.536	1	5.536	686.496
0.2016	25	Ag	10.755	1	10.755	1333.743
0.2016	25	Ag	10.766	1	10.766	1335.082
0.2016	25	Ag	10.047	1	10.047	1245.858
0.2016	25	Cu	59.335	10	593.348	73579.886
0.2016	25	Cu	59.214	10	592.144	73430.518
0.2016	25	Cu	59.884	10	598.843	74261.285
0.2016	25	Ni	142.389	1	142.389	17657.316
0.2016	25	Ni	142.240	1	142.240	17638.852
0.2016	25	Ni	142.435	1	142.435	17663.008
0.2016	25	Zn	420.561	1	420.561	52152.877
0.2016	25	Zn	413.426	1	413.426	51268.130
0.2016	25	Zn	414.991	1	414.991	51462.190
0.2016	25	Pd	0.364	1	0.364	45.188
0.2016	25	Pd	0.369	1	0.369	45.722
0.2016	25	Pd	0.335	1	0.335	41.530
0.2016	25	Cd	0.573	1	0.573	71.007
0.2016	25	Cd	0.485	1	0.485	60.169
0.2016	25	Cd	0.411	1	0.411	51.004
0.2016	25	Hg	0.028	1	0.028	3.522
0.2016	25	Hg	0.078	1	0.078	9.685

Table S5. Initial concentrations of various metal ions in the gold mine wastewater.

Sample volume V (mL)	Fixed volumeV_0 (mL)	Elements tested	Concentration of elements in the test solution C_0(ug/L)	Dilution factor f	Element concentration in the original digestion solution C_1(ug/L)	Element content of the sample C_X(ug/L)
5	25	Au	0.066	1	0.066	0.330
5	25	Au	0.057	1	0.057	0.287
5	25	Au	0.066	1	0.066	0.330
5	25	Ag	2.886	1	2.886	14.431
5	25	Ag	2.899	1	2.899	14.497
5	25	Ag	2.998	1	2.998	14.990
5	25	Cu	12.091	1	12.091	60.457
5	25	Cu	12.472	1	12.472	62.360
5	25	Cu	12.260	1	12.260	61.301
5	25	Ni	7.108	1	7.108	35.540
5	25	Ni	7.302	1	7.302	36.511
5	25	Ni	7.171	1	7.171	35.855
5	25	Fe	139.577	1	139.577	697.887
5	25	Fe	141.808	1	141.808	709.039
5	25	Fe	135.840	1	135.840	679.202
5	25	Zn	29.078	1	29.078	145.391
5	25	Zn	29.842	1	29.842	149.210
5	25	Zn	29.564	1	29.564	147.819
5	25	Pd	0.266	1	0.266	1.332
5	25	Pd	0.313	1	0.313	1.565
5	25	Pd	0.288	1	0.288	1.442
5	25	Cd	0.035	1	0.035	0.173
5	25	Cd	0.052	1	0.052	0.260
5	25	Cd	0.044	1	0.044	0.219

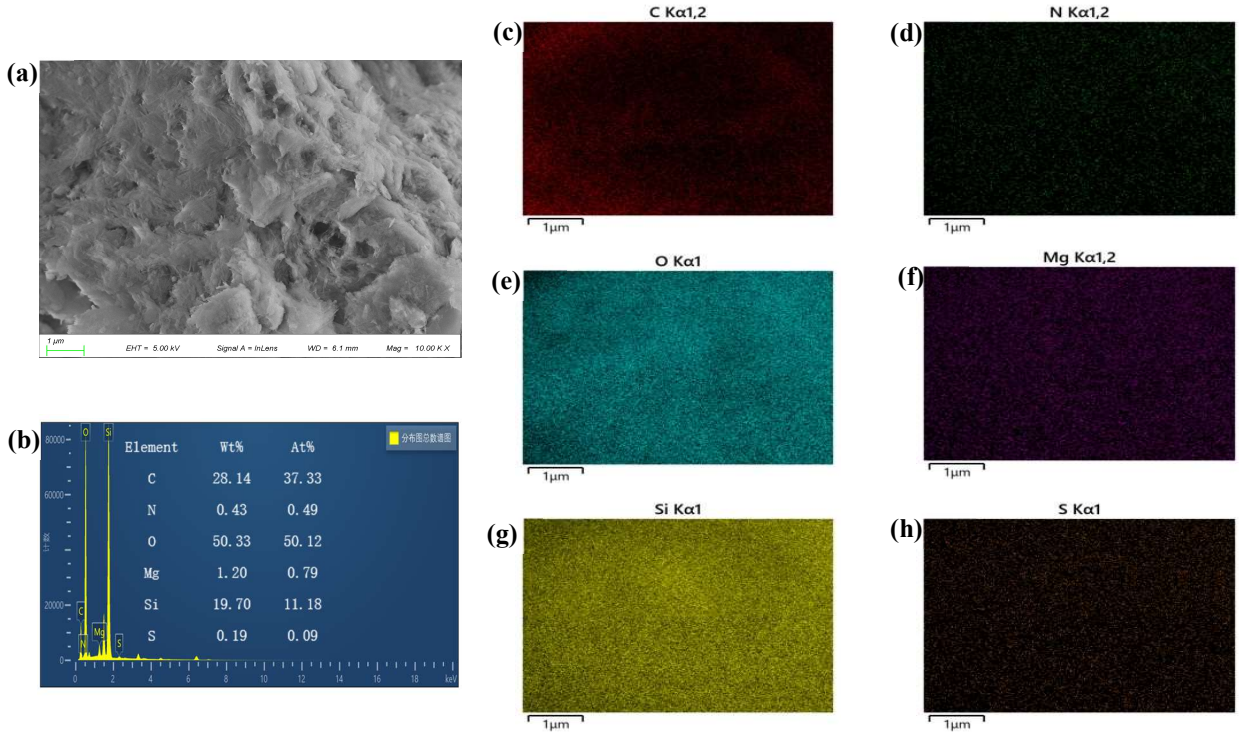

Figure S8 SEM image and corresponding EDS elemental spectrum of HATP.

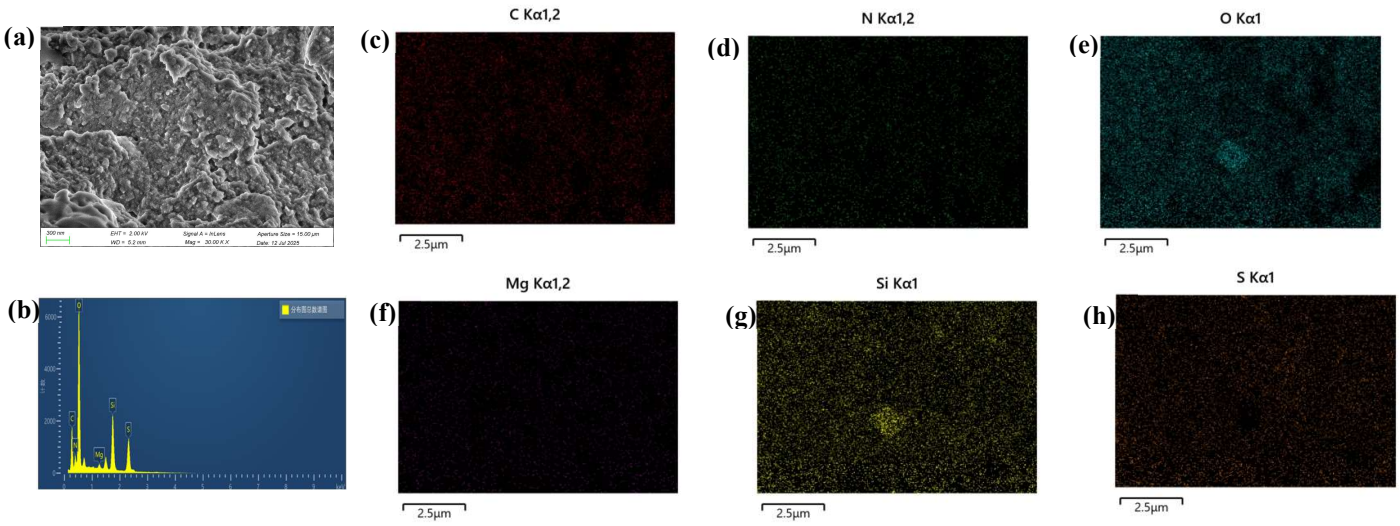

Figure S9 SEM image and corresponding EDS elemental spectrum of Poly(S_5-AM_5)$_5$/$HATP_5$.

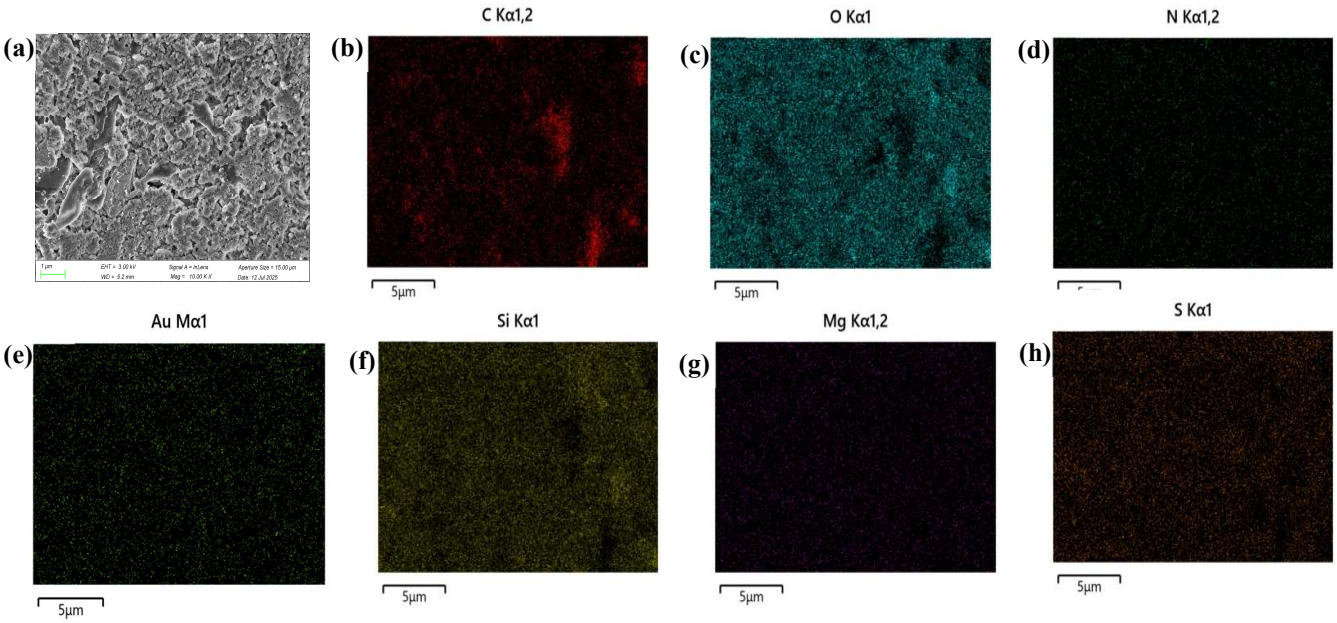

Figure S10 SEM image and corresponding EDS elemental spectrum of Poly(S_5-AM_5)$_5$/$HATP_5$-Au (after Au adsorption).

Table S6. Summary of select studies on noble metal removal by polysulfide adsorbents.

Heavy metal	Adsorbent	q_e (mg g^{-1})	Adsorption Performance over 3 Cycles	Reference
Ag^+	Poly(S-DADMAC)	344	-	Courtney L. Jenkins[2]
	Poly(S-DCPD)	1497	-	Tom Hasell[3]
	Poly(S-Oil mix)	20.98	71.6%	Shi-xiong Wang[4]
Au^{3+}	Poly(S-DADMAC)	602	-	Courtney L. Jenkins[2]
	Poly(S-MCPs)	405-468	-	Ben Zhong Tang
	Poly(S- [VIM]-Br)	636.45	69.52%	Zheng-Jun Quan[6]
	Poly(S-VinI)	1929	-	
	Poly (S-DADM)	845	-	Courtney L. Jenkins[7]
	Poly (S-VTA)	247	-	
	Poly (S-ATA)	48	-	
	Poly(S-AM)/HATP	964.15	96.95%	This work

References

1. J. M. Chalker, M. Mann, M. J. H. Worthington, L. J. Esdaile. *Organic Materials*, 2021, **03**(02), 362–373.
2. M. L. Eder, C. B. Call, C. L. Jenkins. *ACS Applied Polymer Materials*, 2022, **4**(2), 1110–1116.
3. J. Sing M. Lee, D. J. Parker, A. I. Cooper, T. Hasell. *Journal of Materials Chemistry A*, 2017, **5**(35), 18603–18609.
4. Z. Ren, X. Jiang, L. Liu, C. Yin, S. Wang, X. Yang. *J Mol Liq*, 2021, **328**, 115437.
5. J. M. M. Pople, T. P. Nicholls, L. N. Pham, W. M. Bloch, L. S. Lisboa, M. V. Perkins, J. M. Chalker. *Journal of the American Chemical Society*, 2023, **145**(21), 11798–11810.
6. X. Zhou, Y. Cui, X. Xun, J. Jia, X.-C. Wang, Z.-J. Quan. *Separation and Purification Technology*, 2025, **365**, 132679.
7. J. Rollins, C. B. Call, D. Herrera, C. L. Jenkins. *ACS Applied Polymer Materials*, 2025, **7**(13), 8529–8537.